

2

AD-A955 694

August 1962

Project Officer is Interior Report

STARFISH PRIME, *Sanitized Version*

Prepared for

FIELD COMMAND DEFENSE ATOMIC SUPPORT AGENCY
SANDIA BASE ALBUQUERQUE, NEW MEXICO

Contract DA AF-146-92-137

Prepared by Roy J. Leadabrand and Lambert T. Sulphin, Jr

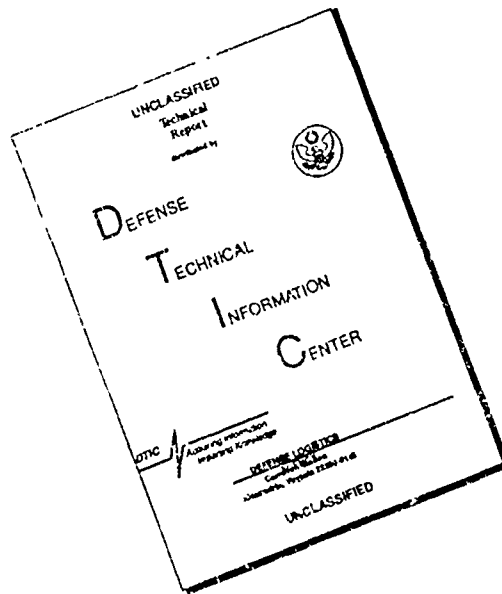
DTIC
SELECTED
JUN 16 1989
S D D
D OS D

Document released under the
Freedom of Information Act.
DMA Case No. 86-90

SRI

DISTRIBUTION STATEMENT A
Approved for public release
Distribution Unlimited

DISCLAIMER NOTICE



THIS DOCUMENT IS BEST QUALITY AVAILABLE. THE COPY FURNISHED TO DTIC CONTAINED A SIGNIFICANT NUMBER OF PAGES WHICH DO NOT REPRODUCE LEGIBLY.

SRI

(4) NA
(5) 829800

August 1962

Project Officer's Interim Report

(6) STARFISH PRIME [redacted] (8)

70
Prepared by
Ray L. Loadbrand
~~Project Officer~~
and
Lambert T. Dolphin, Jr.
~~Alternate Project Officer~~

(7) NA
(9) NA
(11) Aug 62,
(12) 153p
(13) NA
(14) NA

Prepared for:

Field Command, Defense Atomic Support Agency
Sandia Base, Albuquerque, New Mexico

(15) Contract: DA 49-146-XZ-137

(16-19) NA + ok

SRI-2-920

[redacted]

[redacted]

(20) S
(21) NA

[redacted]

[redacted]

QUALITY INSPECTED
2

Accession For	
NTIS Grant	<input checked="" type="checkbox"/>
DTIC TAB	<input type="checkbox"/>
Unannounced	<input type="checkbox"/>
Justification	
By <i>per etc</i>	
Distribution	
Approved for	
Date	23 AX
A-1	

UNANNOUNCED

PHASE SOUNDER
LOG FEROCIC

107 MHz
140 Mc
370 Mc

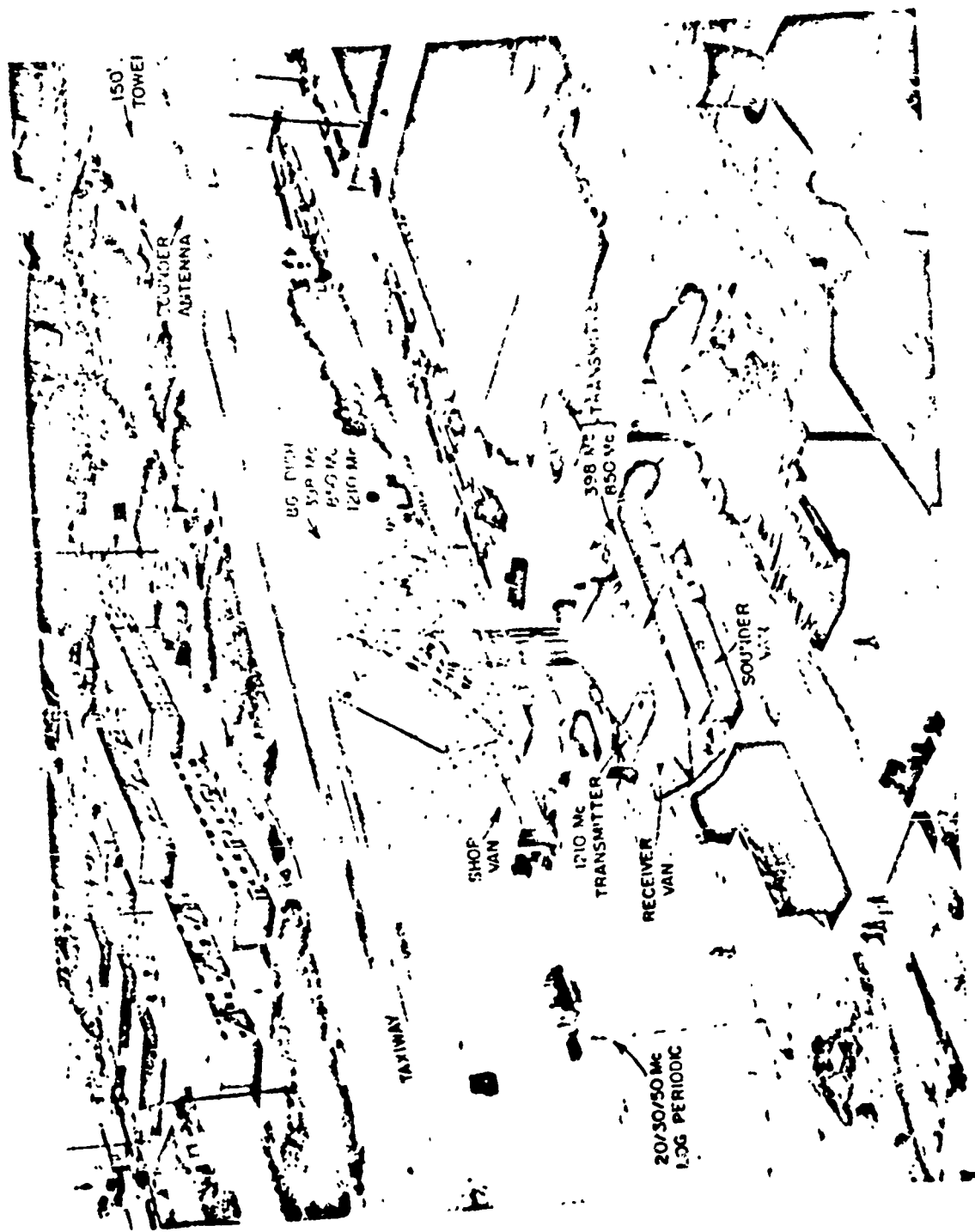
RIOMETER

4 Mc ANTENNA
NOT VISIBLE

ALL-SKY
CAMERA

EQUIPMENT AREAS

11 Mc 32 Mc



JOHNSTON ISLAND RADARS


CONTENTS

LIST OF FIGURES	11
LIST OF TABLES	v
CHAPTER I	
A. Introduction	1
B. Background and Theory	5
C. Instrumentation	11
D. Instrumentation Locations	17
CHAPTER II -- UHF RADAR RESULTS	
A. Burst Area UHF Clutter	29
B. Conjugate Area UHF Clutter.	31
CHAPTER III -- HF AND VHF RESULTS	
A. Equipment Description	36
B. Moving Disturbances -- Johnston VHF Radars	37
C. Johnston PPI Results -- VHF	39
D. Echoes at Great Ranges Seen From Johnston Island.	41
E. Johnston Island HF Results	42
F. Conjugate Area VHF and HF Results	45
CHAPTER IV -- AIRBORNE RADAR RESULTS	
A. Equipment Description	74
B. Location and Geometry	76
C. Results	78
D. Interpretation and Analysis	80
CHAPTER V -- CANTON ISLAND MEASUREMENTS	108
CHAPTER VI -- JOHNSTON ISLAND EARTH-POTENTIAL RECORDS	149
CHAPTER VII -- DAMP SHIP RESULTS.	151
CHAPTER VIII -- CONCLUSIONS	152
REFERENCES	153

[REDACTED]

ILLUSTRATIONS

Frontspiece A	M/V ACANIA	
Frontspiece B	Johnston Island Radars	
Fig. 1-1	Deposition of STARFISH Fission Fragments Model 1: Uncharged Debris	18
Fig. 1-2	Meridian View of STARFISH, Model 3	19
Fig. 1-3	PPI of Possible STARFISH Echoes (from Johnston Island only).	20
Fig. 1-4	Magnetic Field Geometry for STARFISH Burst Area.	21
Fig. 1-5	Magnetic Field Geometry for STARFISH Conjugate Area.	22
Fig. 2-1	Johnston Island UHF Radars	32
Fig. 2-2	STARFISH PRIME - ACANIA Antenna Positions vs Time 370, 140, 32, 11 Mc.	33
Fig. 2-3	STARFISH PRIME - ACANIA Radars, Range-Time Display.	34
Fig. 3-1	Johnston Geometry.	47
Fig. 3-2	Conjugate Geometry	48
Fig. 3-3	STARFISH PRIME, VHF Range-Time Records	49
Fig. 3-4	STARFISH PRIME, Range to Traveling Disturbance	50
Fig. 3-5	STARFISH PRIME, VHF Range-Time Records	51
Fig. 3-6	STARFISH PRIME, Range to VHF Echoes (Johnston Radar)	52
Fig. 3-7	STARFISH PRIME, PPI Radar Display Snapshots 21.050 Mc.	53
Fig. 3-8	STARFISH PRIME, PPI Radar Display Snapshots 28.541 Mc.	54
Fig. 3-9	STARFISH PRIME, PPI Display Snapshots 49.964 Mc.	55
Fig. 3-10	STARFISH PRIME, Geometry for Long-Range Radar Echoes	56
Fig. 3-11	STARFISH PRIME, HF Range-Time Records Johnston Phase-Path Sounder.	57 58
Fig. 3-12	STARFISH PRIME, VHF Range-Time Record 21.050 Mc.	59
Fig. 3-13	STARFISH PRIME, HF Range-Time Record 21.050 Mc.	60
Fig. 3-14	STARFISH PRIME, VHF Range-Time Record 28.541 Mc.	61
Fig. 3-15	STARFISH PRIME, HF Range-Time Record 28 Mc.	62
Fig. 3-16	STARFISH PRIME, HF Range-Time Record 3.358 Mc.	63

[REDACTED]

ILLUSTRATIONS
(cont'd)

FIG. 3-17	STARFISH PRIME, HF Range-Time Record 6.833 Mc	63
FIG. 3-18	STARFISH PRIME, HF Range-Time Record 7.430 Mc	64
FIG. 3-19	STARFISH PRIME, HF Range-Time Record 7.430 Mc	65
FIG. 3-20	STARFISH PRIME, HF Range-Time Record 8.640 Mc	66
FIG. 3-21	STARFISH PRIME, HF Range-Time Record 8.640 Mc	67
FIG. 3-22	STARFISH PRIME, Range to Souther Echoes Johnston Island	68
FIG. 3-23	STARFISH PRIME, ACANIA Radar Range-Time Displays.	69
FIG. 3-24	STARFISH PRIME, ACANIA Phase-Sounder Range-Time Records.	70
FIG. 3-25	STARFISH PRIME, ACANIA Phase-Sounder Range-Time Records.	71
FIG. 3-26	STARFISH PRIME, Range to Souther Echoes Conjugate Area,	72
FIG. 4-1	U.S. Air Force RC-121D.	69
FIG. 4-2	Not used.	
FIG. 4-3	Not used.	
FIG. 4-4a	Abusive 1 Pattern	90
FIG. 4-4b	Lambkin 1-1 Pattern	90
FIG. 4-5	Map Showing Radar Instrumentation Locations for the Study of Clutter Associated with High-Altitude Nuclear Bursts (h = 400 km) STARFISH PRIME.	91
FIG. 4-6	Map Showing Radar Instrumentation for the Study of Magnetic Conjugate Point Clutter Associated with High-Altitude Nuclear Burst (h = 400 km)	92
FIG. 4-7	PPI Display, Abusive 1, at H+2.25 min Prior to Tank-Debris Echo	93
FIG. 4-8	PPI Display, Abusive 1, at H+2.4 min.	94
FIG. 4-9	PPI Display, Abusive 1, at H+2.55 min	95
FIG. 4-10	PPI Display, Abusive 1, at H+9.8 min.	96
FIG. 4-11	PPI Display, Abusive 1, at H+16.4 min	97
FIG. 4-12	PPI Display, Abusive 1, at H+28.4 min	98
FIG. 4-13	PPI and A-Scope Display Between H+0.5 and H+0.85 min.	99

[REDACTED]

ILLUSTRATIONS
(cont'd)

Fig. 4-14	PPI and A-Scope Display Between H=0.85 and H=1.2 min. . . .	100
Fig. 4-15	APS-95 Radar Antenna Pattern in Azimuth Plane in Direction of Echoes.	101
Fig. 4-16	APS-95 Radar Antenna Pattern in Elevation Plane for Azimuth of 279°	102
Fig. 4-17	PPI Display Slant Range vs Magnetic Bearing, H=16 sec, Zero-Degree Off-Perpendicular Contours Shown for Various Heights	103
Fig. 4-18	PPI Display, Slant Range vs Magnetic Bearing H=56 sec, Zero-Degree Off-Perpendicular Contours Shown for Various Heights	104
Fig. 4-19	PPI Display, Slant Range vs Magnetic Bearing, H=66 sec, Zero-Degree Off-Perpendicular Contours Shown for Various Heights	105
Fig. 5-1	Geometry for Canton Observations.	111
Fig. 5-2	STARFISH PRIME, Canton Island Radar Range-Time Display, 27 Mc	112
Fig. 5-3	STARFISH PRIME, Canton Island Radar (cont'd) Range-Time Display 27 Mc.	113
Fig. 5-4	STARFISH PRIME, Canton Island Radar (cont'd) Range-Time Display 27 Mc.	114
Fig. 5-5	STARFISH PRIME, Canton Island Radar (cont'd) Range-Time Display 27 Mc.	115
Fig. 5-6	STARFISH PRIME, Canton Island Radar (cont'd) Range-Time Display.	116
Fig. 5-7	STARFISH PRIME, Canton Radar Echoes 8-9 July 1962, 27 Mc.	117
Fig. 5-8 through Fig. 5-20	All-Sky Camera Photographs, Time Series	118-130
Fig. 5-21 through Fig. 5-33	Ektachrome Photographs, Visual Phenomenon	131-143
Fig. 5-34	STARFISH PRIME, Canton Island All-Sky Camera.	144
Fig. 6-1	Earth-Potential on Johnston Island Developed Across 200-ft Baselines	150

LIST OF TABLES

Table 1-I	Temperature Rise Due to Travel of Fission Debris from STARFISH	23
Table 1-II	Fission-Debris Cloud Radius as a Function of Time	24
Table 1-III	Johnston Island Radar Characteristics	25
Table 1-IV	DAMP Radar Characteristics	26
Table 1-V	AEW Radar Characteristics	27
Table 1-VI	Radars Aboard M/V ACANIA	28
Table 2-1	Johnston Island VHF Radar Clutter Echoes	35
Table 3-1	VHF Clutter Echoes	73
Table 4-1	Parameters of the APS-95 Radar	106
Table 4-11	Locations of AEW Aircraft	107
Table 5-I	Canton Island Radar Characteristics	145
Table 5-II	Chronology of Canton Island Radar Results	146
Table 5-III	STARFISH PRIME Canton Color Photos	148


CHAPTER I


A. Introduction

↓ ho abs
way

The detonation of nuclear devices at high altitudes in the atmosphere produces complex and interrelated phenomena dependent not only on yield, altitude, and ratio of fission-to-fusion yield, but also upon geometry with respect to the earth's magnetic field, and time of day.

The ionizing radiations from the bomb itself produce wide-scale effects which at high altitudes are constrained only by the earth's curvature, the earth's magnetic field and the denser air below. In addition, the lingering fission products are a significant continuing source of ionization effective for many hours. Thirdly, the deposition of large amounts of energy in the atmosphere produces large-scale motions in the atmosphere; shocks, waves, and turbulence, which in the absence of the other two direct ionization effects, would alone be very important in rearranging the natural existing ionization.

There are two separate viewpoints from which radar measurements during high-altitude bursts are important. To answer the immediate needs of systems designers, and to fill in gaps in present knowledge, radar studies of bomb-produced clutter are vitally needed. From the second viewpoint, diagnostic studies are very much in order to improve our understanding of the phenomenon itself. Only through this latter



[REDACTED]

approach can a good body of detailed knowledge evolve which can be drawn upon in the future for systems as yet unconceived.

Previous high-altitude nuclear tests: TEAK, ORANGE, and YUCCA, plus the three ARGUS shots were poorly instrumented and hastily executed. Despite thorough studies of the meager data, present models of these bursts are sketchy and tentative. These models are too uncertain to permit extrapolation to other altitudes and yields with any confidence. Thus there is a strong need, not only for better instrumentation, but for further tests covering a range of altitudes and yields.


Extensive radar clutter from TEAK and ORANGE was observed during HARDTACK/NEWSREEL by Project 6.11 and 6.13 radars (Refs. 1 and 2). There are striking differences between the results observed by these projects, which can only be attributed to the different observing geometry. These differences, plus our good understanding of the radio-reflecting properties of natural aurora, lead one to the belief that much of the bomb-produced clutter is due to ionization which becomes aligned with the earth's magnetic field into long thin columns which scatter anisotropically. Field-aligned ionization is by no means the entire story; absorption, the localized debris cloud, shock waves, and other traveling disturbances complicate the picture so that no single radar location, or single frequency, is adequate to separate the effects observed and to resolve the uncertainties.

To a radius, the sequence of events expected from high-altitude nuclear explosions is somewhat as follows: prior to the burst there

[REDACTED]

will be radar returns only from clutter sources such as aircraft, land masses, or other natural targets. Immediately following the burst, strong absorption will exist for 30-60 sec which will usually preclude receiving returns from the intense ionization produced even at UHF. There will be a decrease in cosmic noise (or propagated atmospheric noise at HF) received by the radars due to this absorption. No changes will be noticed in the returns from low-altitude targets which existed prior to burst, unless of course, one of these targets is a missile or satellite located above 30 or 40 km altitude. The first radar returns at VHF and UHF associated with the burst can be expected to come from the region of the fireball itself. During the early time extremely high ionization densities will fall rapidly. There will be some cross-over for a given frequency and given burst when absorption has decreased sufficiently that radar returns can be obtained, provided that electron densities in the vicinity of the burst then remain sufficiently high. In the case of TEAK, radar returns associated directly with the fission debris permitted tracking of the debris motion at UHF for several minutes, and at HF for several hours. Geometry of the fission debris with respect to the radar is also believed important if such echoes are to be obtained.

The energetic beta particles arising from the primary and secondary sources will be heavily confined by the earth's magnetic field. A great number of these electrons travel to the conjugate point along magnetic lines, producing clutter, auroras, and absorption, in that area as they re-enter the atmosphere and are stopped by collisions.



As the fission cloud slowly decays at a rate approximately proportional to the 1.2 power of time, clutter from the decay beta_s will gradually fall in intensity. The dispersion of the debris cloud, or confinement by the field or by dense surrounding air, will be very important in determining the geographic extent as well as intensity of the clutter. For higher-altitude bursts the debris itself will probably be partially confined by the field lines.

The large scale hydrodynamic motions associated with the high-altitude bursts will severely disrupt the natural state of the ionosphere over a large area. The restoration of natural equilibrium may require twenty-four hours or more, even in the absence of lingering fission debris. Despite well understood physical phenomena, a gap exists because the science of radar physics is relatively young and undeveloped.

Electromagnetic scattering from complex ionized targets must always be considered in research of this nature and poorly-understood mechanisms are often involved. For example, our understanding of the scattering of radio waves from natural aurora or sporadic-E ionization is not yet satisfactory. Despite these difficulties multi-frequency radars are valuable multi-dimensional probes. Wavelength dependence, elevation, azimuth, range, fading rate, Doppler spectrum, amplitude, and time history of the returns from a target all provide information on the target characteristics from which many sound conclusions can be drawn if the data are carefully examined.

[REDACTED]

B. Background and Theory

Before describing the specific equipment used for the FISH BOWL tests, a brief and tentative description of the models for STARFISH will be presented. The models should serve as useful guides in bracketing the extremes of possible behavior. These models are drawn largely from discussions held at Stanford Research Institute in January 1962¹, from re-examination of TEAK and ORANGE Project 6.11 and 6.13 radar data, and from summary documents such as the Electromagnetic Blackout Guide (Ref. 3). Because of the widely divergent opinions as to how STARFISH will behave three distinct models will be outlined.

1. Model 1 - Debris Uncharged² and Remains So

Fission debris and missile fragments will fly radially outward from the STARFISH explosion point essentially unimpeded by the surrounding air. The fission debris products are atoms having masses on the order of half the uranium atom traveling at about 2×10^8 cm/sec (2000 km/sec or 1 percent of the velocity of light). As they travel through the air, they heat it slightly (electron temperature is about 1000°K during pre-dawn hours). Landshoff¹ gives the following figures for temperature rise:

-
1. These meetings were attended by C. Crain, RAND; R. Hendrick, GE TEMPO; R. Meyerott, R. Landshoff, D. Holland and V. Counter, Lockheed; and R. Dyce, R. Leonard, and R. Lundbrand, SRI.
 2. This view supported by Dr. J. W. Bond, Geophysics Corporation of America, Boston, Massachusetts.

[REDACTED]

It is not meaningful to speak of any "fireball" or "rise of the fireball" because the constituents of the shot essentially leave the shot area. The debris which travels upward from the burst will fly outward into space, [REDACTED]

[REDACTED] (This is a measurable quantity.) Upward debris expansion could also be measured optically by observing the radial outward growth using equipment with 0.1 second time resolution.

D x A
(b)(3)

Under the assumption that the debris is uncharged, it will not reach the conjugate point, although fission betas from the fission decay will be compelled to follow the earth's magnetic field. [REDACTED]

[REDACTED]

It can be shown that RF-absorption measurements made through the entire atmosphere are primarily influenced by the beta deposition and not appreciably by gamma effects. On the other hand, VLF waves are reflected from the lower levels of the D-region and so are influenced largely by gamma effects and to some extent by the beta effects. Optical measurements will, on the other hand, be indicative of both beta and gamma deposition. Roughly speaking, for every beta particle, there is a gamma photon from fission debris decay.

[REDACTED]



D4 A
(b) (3)

The layering of the fission debris at altitudes of 110-120 km has caused the STARFISH shot to be occasionally termed the "pancake shot" (Ref. 4).

The foregoing gives the picture immediately after the burst. Thereafter the debris is likely to expand laterally in all directions, in accordance with the behavior of TEAK and ORANGE fission debris. It is uncertain why and how this process occurs. Experimentally observed radial growth rates for TEAK and ORANGE are given in Table i-ii.



2. MODEL 2 - DEBRIS CHARGED

It is unlikely that the debris will be uncharged as was assumed in Model 1. Many theorists feel that charged debris were responsible for many of the phenomena during TEAK, ORANGE, and ARGUS. In fact, experimental confirmation for charged debris traveling along the field comes from the satellite determination of mirror-point distribution of the ARGUS shots. Instead of experimentally observing a distribution consistent with point-injection process, there was found a continuous spread in height, suggesting that fission debris followed the field lines giving off betas as they traveled.³

If charged, the fission debris will travel unimpeded along the earth's field, but will be opposed by the magnetic field when having a component of velocity at right angles to the magnetic field. Actually, the explosion consists of an ionized expanding plasma which will do work against the magnetic field, B, until a volume, V, is displaced which formerly contained a magnetic energy $\left(\frac{B^2}{8\pi}\right)V$ equal to the energy release of the explosion. For STARFISH, this yields a radius of about 1000 km. Thus, a magnetic bubble will be formed restricted in the downward direction by the earth's neutral atmosphere, as in Model 1. There is likely to be a large measure of funneling of debris down the field lines because no work is required in this direction, giving rise to a great deposition of betas well to the north of Johnston Island, but south of French Frigate Shoals.

3. However, a megaton device would result in speeds different by at least a factor of 10 from the debris speeds during ARGUS.

[REDACTED]

Beta deposition directly under the shot, for Models 1 and 2 will be roughly identical. In Model 2, magnetic waves launched by the disturbance of the field will be phenomenal and will be observed as large magnetic perturbations on a world-wide basis. The field pushed aside by the expanding plasma will quickly attempt to collapse, probably breaking through the plasma in an irregular manner analogous to the squeezing of putty between the fingers.

3. MODEL 3 - DEBRIS CHARGED AND EFFECT OF THE MAGNETIZED IONOSPHERE INCLUDED

The magnetic field can be considered as parallel strings under longitudinal tension and lateral compression. In Model 2 we considered the degree to which the earth's magnetic field can contain a megaton explosion. In Model 3, we consider the added effects of the shock wave in the ambient ionosphere as the field lines are displaced. This shock heats up the ionized component of the ionosphere and the ambient electrons acquire sufficient energy to produce, by collision with neutrals, a large scale ionization of the neutral atmosphere. (At night, only 0.1 percent of the air is ionized even at the maximum of the ionospheric F-region.) If the entire neutral component is ionized by the shock, the debris will come to rest at a distance of approximately 30 km in all directions which are at right angles to the field. If this ionizing process is less than 100 percent, the debris would travel further than 30 km before being stopped. This type of expansion process gives rise to a "banana-shaped" plasma bubble, sketched in Fig. 1-2.

[REDACTED]

The X-rays, gammas, and prompt neutrons from the burst shine directly downward, of course, but charged emissions must travel down the field lines, originating wherever the fission debris particles are located. (It is interesting to note that a thermal electron at 1000°K has a gyroradius of 2 cm, a 1-Mev electron has a gyroradius of 80 m, and a typical fission-debris particle, if singly charged, has a gyroradius of about 20 km.)

It is clear that in any model, an area of the D-region located down the field lines from the shot will show profound effects of the shot. There is a wide spectrum of possibilities as to the degree of effects at other areas of the ionosphere near the shot location. Thus the extent of clutter and absorption as well as relative intensities will be important in arriving at a correct interpretation.

Assuming STARFISH behaves roughly according to Model 3, a possible PPI presentation of radar echoes at UHF is shown in Fig. 1-3.

Since the actual experimental results may lie anywhere between the above three models, and since these models hold for early time periods only, further comments on STARFISH models must be postponed until data reduction is completed.

[REDACTED]

C. INSTRUMENTATION

While radar instrumentation for FISH BOWL was hastily conceived and assembled, it is felt that a good assembly of equipment has resulted both at the northern burst area and at the conjugate location.


Briefly, this instrumentation consists of:

- (1) Multifrequency radars at Johnston Island
 - (a) 400-, 800-, and 1200-Mc radars operating into an 85-foot steerable dish
 - (b) 20-, 30-, and 50-Mc radars operating into a rotating antenna
 - (c) Four-frequency sounding radar, in the 4 to 10-Mc band, operating into a vertical looking antenna.
- (2) Airborne 425-Mc radars
 - (a) Two RC 121 D aircraft equipped with 425-Mc Air Early Warning radars will operate in the burst area to map bomb-produced clutter
 - (b) Three similar aircraft will operate in the conjugate area during each event.
- (3) Shipborne radars
 - (a) The M/V ACANIA with research radars will operate in the conjugate area during each event. These radars include a seven-frequency HF sounding radar, and fixed radars at 3, 11, 32, 140 and 370 Mc.

[REDACTED]

Because of the short time scale and relatively limited budget, existing equipment was utilized wherever possible. The Johnston Island UHF radars were assembled using available transmitters used on previous research programs. The M/V ACANIA has been little changed, except for refinements and the addition of the sounding radar, since her participation in HARDTACK. Thus, the equipment and experimental techniques planned for FISH BOWL are proven and reliable.


The Johnston Island UHF radars operate simultaneously into an 85-foot parabolic dish. While it is expected that much of the burst-produced clutter will occur under magnetic field, orthogonality conditions at this point can be resolved only by searching for clutter over large areas of the sky. As mentioned earlier, echoes directly from the debris cloud, and possibly also from regions where large numbers of betas are stopped, may also be observed in addition to "auroral" clutter. For these reasons the 85-foot dish can be operated in a rapid scanning mode, consisting of rapid (6 rpm) rotation in azimuth, with programmed steps in elevation occurring once each revolution. This automatic scan feature can be interrupted at the discretion of the operators to concentrate on particular phenomena. For example, the launch vehicle is usually followed to burst and the antenna poised at the burst until shortly after detonation to ascertain how soon echoes can be obtained in the midst of the expected high absorption levels.



The UHF radars at Johnston Island will provide badly needed data on effects of high-altitude bursts at important systems frequency. Such data are urgently needed for BMEWS, for example, in order to assess the clutter and blackout problems which this system might suffer if the enemy were to deliberately detonate weapons at high altitudes in the BMEWS surveillance area. In terminal defense studies such data are vital to the assessment of the problems of tracking incoming warheads and discriminating against decoys in an environment where high-altitude bursts have occurred or are occurring.

During HARDTACK good radar data were obtained only as high as 125 Mc. The three UHF radars utilize modulating anode klystrons to develop approximately 40 kw of peak power. The cathodes of these tubes permit operation at long pulses if desired, although operation at 100 to 300 μ sec pulses, and PRF's of 75 to 150, is likely during PISA SOWL. Receivers are preceded in each case by parametric amplifiers to improve sensitivities and hold noise figures to 4 db or less.

Lower frequency radars at Johnston Island have been included to provide long-term tracking of fission debris and information on the disturbed ionosphere. Radar frequencies at 20, 30, and 50 Mc will primarily be used for tracking of the fission debris. These radars consist of three exciters sequentially fed into a 30-kw distributed-line power amplifier. A common rotating log-periodic antenna is used. This same final amplifier is also used for the lowest four




radar frequencies, which can be adjusted anywhere in a band extending from 4 to 10 Mc. A filter is used to divert the 4 to 10-Mc frequencies into a vertical log-periodic antenna. Table 1-III is a summary of the characteristics of the Johnston Island radars.

Data from all radars will be recorded on magnetic tape together with antenna position and timing information, as well as voice comments and auxiliary data. Backup film recording will be used, and PPI photographs will be taken in real-time to provide continuous surveys of results and immediately available data.


The project also operates an all-sky camera and earth potential recorders at Johnston Island. The camera, a type developed for auroral photography, provides a wide angle view of the entire sky. The earth potential records provided information on the direction and relative intensity of induced currents flowing in the ground which result from charge motion in the ionosphere.

Early in the planning of radar instrumentation for FISH BOWL it was realized that participation of the USAS AMERICAN MARINER with her precision tracking radars would add valuable instrumentation to the operation and fill a geographical gap by providing a radar platform at sea in the burst area. The AMERICAN MARINER, also known as the DAMP ship (for Downrange Anti-Missile Program), is operated for ANPA and AOMC by RCA. This ship has been engaged for the past three years in missile re-entry investigations on the Atlantic Missile Range. Because of ANPA's interest in nuclear effects, the ship's normal missile re-entry program was interrupted to permit participation in FISH BOWL. Although originally considered a part of



Project 6.9, a separate project number (6.13) was later established because of the different logistics and contractual requirements for the two operations. The DAMP ship radars consist of two C-band AN/F1Q-4 precision trackers, and an L-band and a UHF radar (with common 30-foot dish) which can be slaved to either F1Q-4 tracker. Table 1-IV is a summary of the DAMP radar characteristics. In addition to clutter investigations, the DAMP ship obtains data on scintillation and angular deviation effects. To accomplish this, seven rockets (launched from Johnston Island) carrying C-band beacons are tracked during each event by one of the C-band radars. The remaining radars investigate the extent of the bomb-produced clutter.

Since neither the burst nor its conjugate area can be adequately studied from a single radar location, additional radars are required if valid conclusions are to be possible. The deficiency of nearby land masses in either area makes it nearly impossible to provide adequate coverage without mobile platforms. Project 6.13 employed an experimental AEW aircraft during TEAK and ORANGE and were highly successful. Since 1958 this airborne radar system has become operational with the Air Force to fill gaps in land-based AEW networks. Mounted in Lockheed KC 121 D (Super-Constellation) aircraft, these radars



are highly sensitive and relatively flexible, hence are well suited for nuclear clutter measurements. Characteristics of the radars are outlined in Table 1-V.

Data is recorded aboard the five AEW aircraft photographically. In addition to photographing the PPI display, echo amplitude is recorded by photographing the A-scope presentation.

The M/V ACANIA, to be operated as primary instrumentation at the conjugate location during FISH BOWL, was originally outfitted for participation in HARDTACK in 1958. The ship houses radars which cover the spectrum from low HF through 370 Mc, at twelve discrete frequencies. Radar characteristics are outlined in Table 1-VI. Data are recorded on magnetic tape from which a variety of film or pen-chart records can be made. Timing and antenna position information are also recorded on tape. The ship houses data reduction facilities and is capable of operating on the open sea except during severe weather. An all-sky camera will also be operated aboard the ship.



D. Instrumentation Locations

It is important that research radar equipment be placed in the burst and conjugate areas in enough different locations to assure that the clutter areas are adequately covered, so that the extent of the disturbed regions can be determined, to provide variable geometry with respect to the ionized areas, and to ascertain the significance of field confinement and geometrical properties of the scattering centers. Project instrumentation for FISH BOWL has been placed with these points in mind. Primary instrumentation was first located at Johnston Island. The M/V ACANIA was then placed in the conjugate area along a magnetic meridian from the burst, and such that the ship's radars can look south perpendicular to the field lines at about E-region heights. Contours of orthogonality were then drawn for both locations and four AEW aircraft placed so that either occurrence or non-occurrence of echoes is significant.

Figures 1-4 and 1-5 are maps showing the locus of points perpendicular to the field for each transmitter location, for which field-aligned echoes would be possible.

PAGES 18-22 DELETED

[REDACTED]

TABLE 1-1

TEMPERATURE RISE DUE TO TRAVEL OF FISSION DEBRIS FROM STARFISH

DNA
(A) (S)

[REDACTED]

[REDACTED]

[REDACTED]

TABLE 1-11

FISSION-DEBRIS CLOUD RADIUS AS A FUNCTION OF TIME

DWA
(6) (3)

[REDACTED]	[REDACTED]	[REDACTED]
[REDACTED]	[REDACTED]	[REDACTED]
[REDACTED]	[REDACTED]	[REDACTED]

[REDACTED]

TABLE 1-III

JOHNSTON ISLAND RADAR CHARACTERISTICS

Radar	Frequency (Mc)	Wavelength (m)	Peak Power (kw) ¹	Antenna	Antenna Gain (db)	Antenna Beamwidth ²
1	1210	0.25	40	Common 85-foot steerable dish	48	0.75
2	850	0.35	40		45	1.1
3	403	0.74	40		38	2.3
4	50	6.0	30	Common rotating log-periodic	9	
5	30	10.0	30		6-9	60 x 60
6	20	15.0	30	Vertical log-periodic	3-6	60 x 90
7-10 ³	4-10	75-30	30			

¹ Typical operating conditions 150 PRF, 300 usec pulse

² One-way half-power antenna beamwidth

³ Four adjustable frequencies

TABLE 1-IV
DAMP RADAR CHARACTERISTICS

<u>Radar</u>	<u>Frequency (Mc)</u>	<u>Peak Power (kw)</u>	<u>Pulse Width(μsec)</u>	<u>Antenna</u>	<u>Antenna Beamwidth(°)</u>
1	3450-3800	2.5	1	15-foot dish	0.86
2	3450-3800	2.5	1	15-foot dish	0.86
3	1300	2.0	2	Common 30-foot dish	2
4	125-530	2.0	2		6

* One-way, half-power

TABLE 1-V
 AEW RADAR CHARACTERISTICS

<u>Frequency (Mc)</u>	<u>Peak Power (Mw)</u>	<u>Average Power (kw)</u>	<u>Pulse Width (μsec)</u>	<u>PRF</u>	<u>Antenna Beamwidths (°)</u>
425 ±5	2.0	3.8	6	300	8.2 horizontal 36 vertical

TABLE 1-VI
RADARS ABCARD R/V ACANIA

<u>Frequency (Mc)</u>	<u>Peak Power (kw)</u> ³	<u>Antenna</u>	<u>Antenna Gain (db)</u>	<u>Antenna Beamwidth</u> ¹
370	50	30-Foot Dish	30	5
40	40		21	13.5
32.5	100	8-Element Yagi	12	45
2.1-2.5	7	3-Element Beam	3	60
4.76	7	Dipole	3	50
3 - 30 Mc	30	Vertical Log-Periodic	3 - 6	60 x 90

1. One-way half-power beamwidth
2. Seven adjustable frequencies, phase coherent
3. Typical operation - 30 PAF, 300 μ sec pulse

[REDACTED]

CHAPTER II UHF RADAR RESULTS

A. Burst Area UHF Clutter
by Ronald Pressnell

The UHF clutter radars located on Johnston Island were operated for several hours prior to the bomb burst and for seven hours following the bomb burst. The equipment characteristics are described in Chapter I-C. Prior to the burst, the radar executed a programmed track of the Thor launch, and the 850- and 1210-Mc radars obtained skin echoes during the entire trajectory. Shortly before the burst the antenna was positioned to look in the direction of 87 degrees elevation and 190 degrees azimuth, which is approximately 2 degrees higher in elevation than the burst direction. At burst, [REDACTED]

DNA
(b)(3)

[REDACTED] The 398-Mc transmitter was turned on at burst and apparently was not up to power in time to see these same echoes. During the next 1,000 seconds many echoes were observed on all three radars. Figure 2-1 is a display of the antenna position, and range-time displays of the three UHF radars. The great majority of these echoes appear to be caused by ground clutter and small rocket debris, as well as tankage debris. The echoes which appear to be due to burst effects are listed in Table 2-1.

From H+120 sec to about H+3,000 sec the antenna was executing a programmed scan. Following H+3,000 sec the antenna was positioned at magnetic north and 50 degree elevation, or was periodically scanned.

[REDACTED]

[REDACTED]


[REDACTED]

DNA
(b) (3)

[REDACTED]

No effects were observed during the sodium-flare launching the following morning.

[REDACTED]


B. Conjugate Area UHF Clutter
by Lambert Dolphin, Jr.

Radars at 140 and 370 Mc aboard the M/V ACANIA in the southern conjugate area obtained radar returns for brief periods after the detonation. These returns were confined to the magnetic south and appear to have satisfied the orthogonality conditions for reflection from field-aligned ionization.

The ACANIA's 30-foot dish was scanned in a complex manner throughout the test; antenna azimuth and elevation vs. time are shown in Fig. 2-2.

Range-time records prepared from magnetic tape are presented in Fig. 2-3 for the period H=0 to H+10 min. All of the southern UHF echoes appear to have occurred in this time interval.

Almost immediately after H=0 four individual radar returns spaced 1/30 of a second apart were seen on the 140-Mc radar at a range of 150 km. These echoes were evidently due to electrons from the burst passing down the burst field line into the conjugate area.

Radar clutter echoes followed at 140 and 370 Mc for brief periods as the antenna scanned past 60-degree elevation and 191-degree azimuth. At 370 Mc these echoes occurred between 0901:00 and 0903Z and at 140 Mc from 0901:00 to 0904:10Z. Range to all echoes was 150 to 180 km. Records beyond H+15 min have not yet been examined at these frequencies.

The 32.5 Mc Range-time record is also shown in Fig. 2-3. This record is discussed in Chapter 3.



CHAPTER III HF AND VHF RESULTS

by

Lambert T. Dolphin, Jr.

A. Equipment Description

HF and VHF radars were operated both at Johnston Island and aboard the ACANIA in the conjugate area during STARFISH Prime. At Johnston Island this equipment consists of a seven-frequency phase coherent sounder, providing 10 kilowatts of peak power output (200 microseconds pulses), at seven frequencies which remained fixed during the test. The lowest four frequencies (3.3, 6.8, 7.4, and 8.6 Mc) operated into a log-periodic antenna mounted vertically on a 150-foot tower. The remaining frequencies 21.050, 49.964, and 28.541 Mc operated into a horizontal log-periodic antenna which was rotated at 2 rpm.

Aboard the ACANIA is a similar seven frequency antenna with frequencies set to 4.7, 5.6, 6.66, 7.92, 9.63, 13.82, and 20.0 Mc. The ACANIA also possesses radars operating at 3.3, 11.15, and 32.5 Mc. Peak powers at these latter frequencies are approximately 4, 7, and 100 kw, respectively. A simple dipole is used at 3.3 Mc, a 3-element beam at 11.15 Mc, and an 8-element beam at 32.5 Mc. The sounder antenna on the ACANIA is similar to that at Johnston, except that the tower is half as high.

Geometry of the Johnston Island radars is shown in Fig. 3-1 and the corresponding ACANIA geometry for the conjugate area is shown in Fig. 3-2.

[REDACTED]

B. Moving Disturbances--Johnston VHF Radars

[REDACTED]
[REDACTED]
[REDACTED]. No echoes corresponding to these echoes were observed in the conjugate area by the ACANIA, using similar frequencies, indicating that the disturbance was probably unique to the burst location.

(6) + 17
(5)

Figure 3-3 is the range-time record which exhibits these echoes. Range to these earliest traveling echoes is plotted in Figure 3-4. In an attempt to explain these echoes it was first hypothesized that the echoes were associated with a horizontally traveling disturbance near the F-layer maximum. The data was then replotted to show true disturbance velocity horizontally as a function of time. Velocities from the resulting plot appear to be associated neither with the slow magneto-acoustic, nor the fast MID waves. In addition velocities increased with time result. The first hypothesis was therefore discarded. A second hypothesis is that the radars observed motion of ionization directly upwards, perhaps due to debris escaping directly overhead. Or thirdly, the motion of debris up the field lines toward the conjugate area may have been observed. [REDACTED]

[REDACTED] and no modulation of the echoes by antenna rotation was seen for the first several minutes so that the echoing area must have been nearly overhead and moving with a large vertical component of velocity.

[REDACTED]

[REDACTED]

These echoes were modulated by antenna rotation although it has not yet been determined if maximum echo intensity occurred to the south.

Following these early moving echoes which receded in range away from the radar, echoes approaching the radar, and apparently unrelated to the preceding echoes were seen. From the PPI photographs it appears that these later echoes moved in from the south, passed overhead, and were followed by auroral echoes of long duration to the north. [REDACTED]

John
(M) (S)

[REDACTED]

[REDACTED]. Figure 3-6 is a plot of the range to all moving echoes vs. time. (On this plot, the echoes at great range which do not move significantly in range are discussed in Sec. 4). Virtual velocity (not considering geometry or group retardation) is indicated on the plot.

Prior to approach and passage of the disturbance which moved in from the south, [REDACTED]

[REDACTED]. This leads to the speculation that the clutter to the north was somehow related to the echoes which moved in from the south and passed overhead. It seems difficult to ascribe these results to debris motion at such late times after burst, but this is the mechanism which occurs to the authors, in the absence of other data inputs.

[REDACTED]

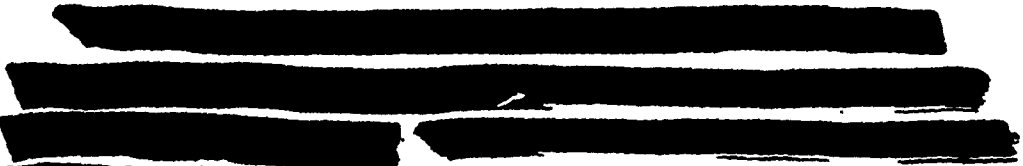


C. Johnston PPI Results--VHF



Into the normal magnetic tape recording of the receiver outputs, a PPI oscilloscope was photographed in order to present radar returns vs. azimuth and range. Selections from these PPI films are shown as Figs. 3-7, 3-8, and 3-9. Table 3-1 is a compilation of the times and durations of the northern radar clutter echoes seen at each frequency.

(S) D+A
(S)




It can be seen that this echo is due to a disturbance traveling towards Johnston Island. (See also Chapter II) Perhaps motion of debris down the field lines towards the radar would account for these echoes. The relatively high elevation angle to the field lines in question is consistent with the broad spread in azimuth of the observed targets.

Except for this one moving disturbance all of the PPI records show in general echoes at ranges less than 500-km range, skewed to magnetic north. Ground reflected multiple echoes are also present at times.

The disturbance which was seen receding from the radar (20 and 50 Mc) on the range-time records between 0901 and 0904Z was too weak to be seen





on the PPI records, since the range-time presentation gives considerable film integration.

PPI recordings were taken from 0 to 1500 km only; hence, echoes seen on range-time records beyond 1500 km were not seen on the PPI display.

D. Echoes at Great Ranges Seen From Johnston Island

In addition to moving disturbances and close-in clutter, the 20- 30- and 50-Mc radars at Johnston also obtained radar reflections [REDACTED]

[REDACTED] These echoes are visible on the range-time records, Fig. 3-5. [REDACTED]

[REDACTED] Figure 3-10 is a sketch of the large-scale STARFISH PRIME geometry which should aid in interpreting these far out echoes. [REDACTED]

[REDACTED] reflections from the southern auroral region could have been seen at Johnston. It is also possible that reflections from the debris tube were involved. [REDACTED]

Interpretation of these echoes should be simplified when the Canton 27-Mc radar records have been examined more completely.



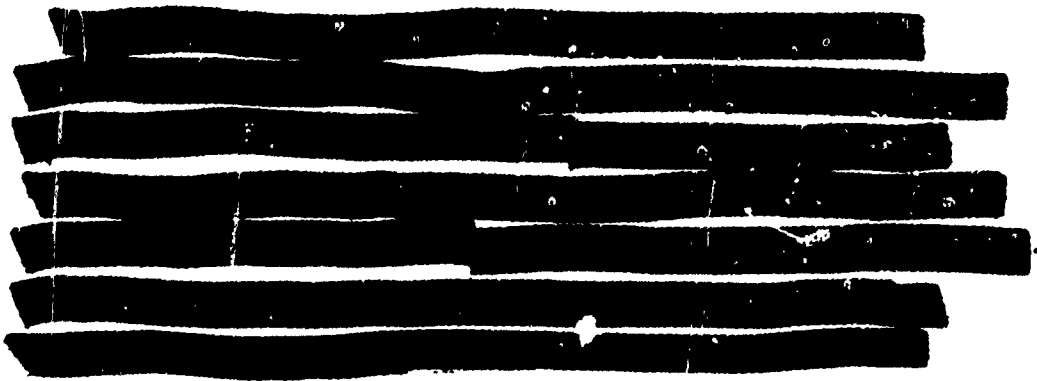
E. Johnston Island HF Results

The Johnston seven-frequency phase-path sounder was set for operation at the fixed frequencies:

- | | |
|-----------|--|
| 3.358 Mc | } Vertical log-periodic antenna |
| 6.833 Mc | |
| 7.430 Mc | |
| 8.640 Mc | |
| 21.050 Mc | } Horizontal rotating log-periodic antenna |
| 49.964 Mc | |
| 28.541 Mc | |

While features of the 20/30/50 Mc records have already been discussed under VHF clutter effects, there is useful F-region ionospheric data in these records as well, just as those three frequencies provide data which is transitional to the UHF clutter data.

Range time records of the seven sounder channels are presented as Figs. 3-11 through 3-21. Except for a few special points along these records, a cursory examination suffices to pick out the highlights.



D x H
(6) (3)






Range to the leading edge of all echoes at each sounder frequency is plotted in Fig. 3-22 as functions of time. From the HF records we conclude that a new F-layer formed presumably as a result of the ionization from debris decay. (It is assumed that the original F-layer was largely swept out of the Johnston Island area by the action of the sonic magneto-acoustic wave, which had proven large effects (i.e., lowering F-region critical frequencies) at many distant stations. Another argument for existence of a new F-layer target is the fact that even the early post-burst echoes obtained at the lowest four frequencies were coherent on a pulse to pulse basis, while the early 20/30/50 Mc early auroral echoes were not.

D 44
(4) (5)





The character of the echoes from the new F-layer became more diffuse at all four low frequencies beginning about 1105Z, when the layer height began to fall. (Diffuseness here indicates an increase in range depth of the echoes.)

HF data was collected throughout the day following STARFISH PRIME but has not yet been examined due to time required for running film records from magnetic tape.

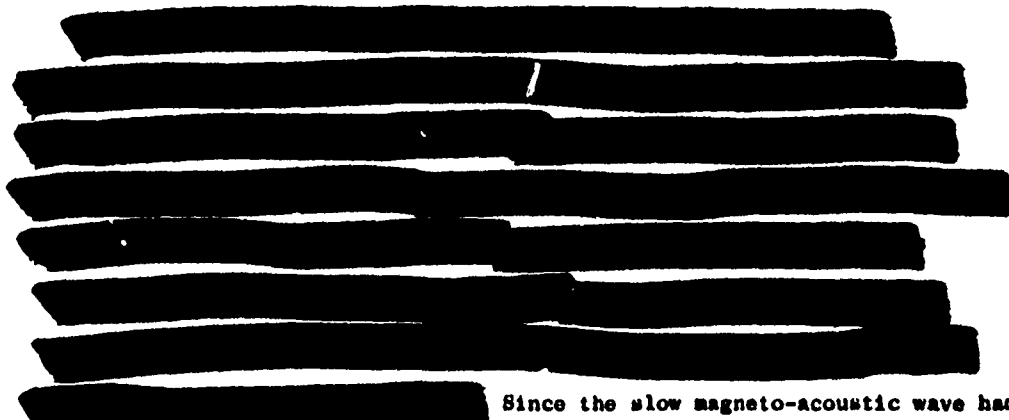


F. Conjugate Area VHF and HF Results

Radars aboard the ACANIA at 3.3, 11.15, and 32.5 Mc, as well as sounder frequencies of 4.7, 5.6, 6.66, 7.92, 9.63, 13.82, and 20.0 Mc, provided data for many hours after STARFISH PRIME. Like similar data in the northern area, this data concerns (1) long-lasting field-aligned clutter, and (2) the disturbed ionosphere in the conjugate region.

Figure 2-3 contains the 32.5-Mc radar early range-time records. Figures 3-23 through 3-25 are early range-time records for the remaining frequencies. Because of the long times required to run range-time films from magnetic tape, all the records have not been run in time for this report.

DNA
(1)(3)



Since the slow magneto-acoustic wave had not yet arrived at the conjugate area, the overhead echoes may have been due to the normal pre-shot F-layer, seen after absorption fell to sufficiently low values.



[REDACTED]

[REDACTED]

DNA
(2) (3)

Radar receivers on the ACANIA were saturated for many hours by the intense echoes.

[REDACTED]

While a quantitative estimate of the differences in northern and southern area clutter is not yet possible, it seems quite clear that the late time southern clutter was definitely more extensive and intensive than that seen from Johnston.

PAGES 47-73 DELETED

[REDACTED]



CHAPTER IV AIRBORNE RADAR RESULTS

by
Walter E. Juye

A. Equipment Description

The five RC 121-D aircraft participating under Project 6.9 in Operation FISH BOWL belong to the 552nd AEW and C Wing at McClellan Air Force Base. For this operation this detachment was under the command of Lt. Col. H. T. Wagnon.

These aircraft are modified Lockheed Super Constellations (C 121). Their normal function is the patrolling of the U. S. coast line in order to detect any penetration of the ADIZ by unidentified aircraft. They operationally report to the Air Defense Command. In order to perform their normal mission they are equipped (Fig. 4-1) with the APS 45 X-Band height-finder radar and the APS 95 UHF search radar. In addition to their normal navigational equipment, these aircraft carry five ARC 27 UHF transceivers and two 618 S1 high-frequency AM transceivers. The aircraft is capable of up to 17 hours in the air and carries between 14 and 18 crew members on a normal mission.

For the purposes of Operation FISH BOWL only the APS 95 UHF radar was used. The parameters of this radar are shown in Table 4-1.


* Note: Figs. 4-2 and 4-3 were not used.

[REDACTED]

Three of the five airplanes participated in Operation DOMINIC at Christmas Island. For this mission a 618T single-sideband HF transmitter was installed in these aircraft so that they would be able to receive the countdown, and the remaining two aircraft were equipped by Stanford Research Institute with Collins 75S1 single-sideband HF receivers.

These aircraft are normally equipped with PPI-scope cameras taking pictures at the rate of one frame per antenna revolution.

A heading marker appears on the oscilloscope each time the beam sweeps past the nose of the aircraft. The scopes are north-magnetic stabilized. For the purposes of Operation FISH BOWL, SRI equipped the five aircraft with A-scope cameras which were mounted on the 5-inch A-scope normally used to monitor various functions of the radar. The A-scope also took one frame per antenna revolution, thus integrating the amplitude vs. range information over the full 360-degree sweep.



B. Location and Geometry

For each test Project 6.9 had requested five aircraft such that two would be airborne in the southern conjugate area, two airborne in the northern burst area, and one airplane used as backup at Hickam. Because of the large number of aircraft in the airborne array around Johnston Island and because of the difficulties experienced in controlling such an array during the BLUEGILL rehearsals, T.G. 8.4 requested from T.G. 8.1.3 that the fifth aircraft be made available to T.G. 8.1 during the tests so that it could serve as primary airborne control aircraft. Because of the "no go" condition imposed on the test if both Project 6.9 aircraft in either the northern or southern area were grounded or had to abort, it was agreed that the airborne control aircraft would assume the primary position assigned to one of the two Project 6.9 aircraft in the northern area if neither plane could be on station at the time of the test.

For STARFISH Prime the aircraft were located as shown in Table 4-II. T.G. 8.4 code names for the aircraft were as follows: Abusive 1 was the airborne control aircraft; Lambkins 1 and 2 were aircraft in the northern burst area; and Lambkins 3 and 4 were aircraft in the southern conjugate area.

[REDACTED]

The location and flight pattern (Fig. 4-4a) of the Abusive aircraft was determined by its airborne control function. The four Lambkin aircraft flew a pattern as shown in Fig. 4-4b. The choice of pattern was based on the following considerations:

- (1) In order to remain as close as possible to the center point of the station but still have the aircraft fly in a straight line for a reasonable length of time (radar data unusable during turns), a compromise value of 5-min. legs was chosen.
- (2) Because clutter echoes were expected primarily in the magnetic east and west and because the antenna pattern of the APS 95 is quite favorable at the 90- and 270-degree bearings from the aircraft, the pattern was established along the magnetic north-south line.

At the time at which the coordinates of the aircraft stations were decided upon, it was felt that the fission debris from the STARFISH burst would be, in the extreme dispersive case, deposited in the E-layer under the shot location in pancake fashion (see Model 2, p. 20, Pre-test Report^{*}). The aircraft were then located such that they would give a measure of the geographic extent of the debris spread vs. time after burst (Figs. 4-5 and 6). The reason for the lateral offset (eastward shift) is that the APS 95 airborne radar is limited to 20 degrees in elevation which requires a minimum ground range of 260 km to observe targets at a height of 100 km.

^{*}Leadabrand, R.L. and Dolphin, L.T., "Radar Measurements During FISH BOWL" Pre-test Report, Operation FISH BOWL, TU 8.1.3, Project 6.9 SRI, Menlo Park California, April 1962 [REDACTED]

[REDACTED]

C. Results

1. Radar

Observed radar results are similar to those postulated by the Model 3 on the Pre-Test Report. The ionized debris funneled considerably to the north and south conjugate areas. Hence, minimum clutter effects were observed by the aircraft.

[REDACTED]

DNA
(b)(3)

2. Visual Observations

Weather conditions in the northern area were as follows:
Abusive 1, flying at 13,000 ft, had scattered cirrus clouds. Lambkins 1 and 2, flying at 10,000 ft, had fairly thin, hazy overcast. In the southern area Lambkins 3 and 4, flying at 15,000 ft, had no overcast. Optical results as reported by various observers in these aircraft were spectacular.

[REDACTED]

*Leadabrand, R.L. and Dolphin, L.T., "Radar Measurements During FISH BOWL [REDACTED] Pre-Test Report, Operation FISH BOWL, TU 8.1.3, Project 6.9 SRI, Menlo Park, California, April 1962 [REDACTED]"

[REDACTED]



[REDACTED]

[REDACTED]. This band had a "chartreuse" inner streak.

[REDACTED]

[REDACTED] The wide band faded through deep pink to pale pink, with the center streak becoming fainter, whiter, and wider.

[REDACTED]

[REDACTED]

[REDACTED]

[REDACTED]

DNA
(6) (3)

Lambkin 1 at position S2, flying a magnetic south track at the time of the burst, reported a white band extending from the burst area as far south as could be detected through the clouds, with two or more additional white bands appearing to be on top of the brightest one. Lambkin 2 in position S1 also reported yellow-white "fingers" extending to the south magnetic horizon. Lambkins 3 and 4 in the southern conjugate area, flying on a magnetic north track at the time of burst, both reported the presence of red glow in the south and slightly west of them. A bright streak extended from horizon to horizon north to south, breaking up into finger-like streamers in the northern horizon.

[REDACTED]

[REDACTED]

[REDACTED]

[REDACTED]

[REDACTED]

[REDACTED]

[REDACTED]

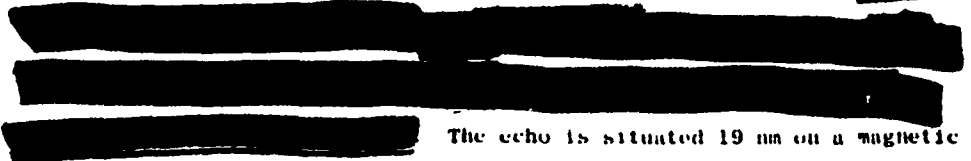




D. Interpretation and Analysis

1. Abusive 1 Data

At the time of the burst, Abusive 1 was located 80 nm slightly north of east of ground zero on a true heading of 330 degrees.



The echo is situated 19 nm on a magnetic bearing of 180 degrees from Johnston Island which is essentially the location of ground zero. The position of this echo with respect to the burst, the duration of the echo, and the geometry of the radio ray with respect to the magnetic field are such that we speculate that these echoes originate from the Thor tankage debris located essentially directly below the burst at an altitude between 40 and 50 km. The time of onset of this echo is commensurate with the time it would take for the tankage to reach this altitude and to break up if it were not already broken up due to the effects of the detonation. The duration of this echo is also well within the limits of previous observations on the Atlantic Missile Range by both UHF radars (370 Mc) and C-band radars. Pictures of the detonation have shown that at least the surface of the tankage was heated to very high temperature when it was reached by the blast or debris wave. To the best of our present knowledge there was no evidence of the tankage breaking up at that time although it appears to be safe to surmise that the tankage was structurally weakened from the effects of both the X-rays and the debris impingement. The tankage in any case would not survive re-entry.

DNA
(6) (2)



[REDACTED]

2. Lambkin 1 Data

[REDACTED]

[REDACTED] Figures 4-13 and 14 show PPI and A-scope presentations simultaneously, starting with Frame 93 at H+0.5 min. Note that the clock on the PPI film is fast by 2.5 min. The heavy line across the echo on the A-scope display is due to the "folding over" of the peak of the echo because of receiver saturation. Saturation effects are also noticeable in the sea clutter echoes as seen in the A-scope. On the PPI display, particularly on Frame 94, a darkened area between the sea clutter and the echo is due to the decrease in noise which sometimes occurs when the receiver saturates. The antenna pattern in the direction of the echo is shown in Figs. 4-15 and 16.

D+A
(b) (5)

The echoes observed extend over a large geographical area. For discussion purposes assume that these echoes were field-aligned. Zero-degree off-perpendicular angles were computed for the magnetic bearings at which the echo exists and for heights of 80, 100, 120, and 150 km (Figs. 4-17, 18, and 19).

[REDACTED]

[REDACTED]

[REDACTED]

[REDACTED]

[REDACTED]

[REDACTED]

[REDACTED]

[REDACTED]

* Dolphin, L. T., and Dyce, R. B., "Operation HARDTACK/NEWSREEL Radio Attenuation on Reflection Phenomena", SRI Proj. 2445, Final Report, Part I, AFRCR-TR-60-105, p 35, Stanford Research Institute, Menlo Park, California (February 1960)



[REDACTED]

The actual picture is more complex since the antenna pattern is not a rectangular block but more banana shaped.

[REDACTED]

DNA
(b)(3)

For the purpose of obtaining a quantitative value of cross section of the echo, let us assume that the target was essentially a point.

[REDACTED]

More realistically one has to assume that the target was beam-filling in the azimuth plane. If the scattering region is indeed field-aligned, one must then make assumptions on the scattering efficiency and on the vertical



[REDACTED]

extent of the echoes before one can compute radar cross sections.

If one were to assume that the target filled the whole beam, one can then compare the cross section of a point target to the volume in the beam.

[REDACTED]

3. Possible Hypotheses to Explain Results on Lambkin 1

1. Hypothesis 1

At very early times, X-rays and gamma rays cause ionization at many altitude levels.

DNA
(b) (3)

[REDACTED]

Peterson, A. M., "Radar Clutter Effects of High Altitude Nuclear Explosions," AMRAC Proceedings, Vol. IV, Part 1, Institute of Science and Technology, The University of Michigan, Meeting of 8-10 May 1961, Colorado Springs, Colorado, p 847 [REDACTED]

Advanced Research Projects Agency, "Report on Nuclear Interference," Advanced Research Projects Division, Institute for Defense Analysis, Contract SD-50, IDA ARPA, TR 60-3.

[REDACTED]

[REDACTED]

a. Pro and Con Arguments

(1)

[REDACTED]

(2) X-rays, if not included in TEMPO's work, may cause additional ionization which would cause additional absorption.

[REDACTED]

Their energy is deposited higher so absorption per free electron produced is less effective.

(3) Barometers on Johnston Island pinned

[REDACTED]

for a minute or so before swinging positive due to synchrotron radiation.

b. Summary

Though detailed numbers must be calculated and more data accumulated from other projects,

[REDACTED]

[REDACTED]

[REDACTED]

DNA.
(b)(3)

+ Hendrick, R. W., Christian, R. M., Fischer, P. G., "Operation FISH BOWL

Estimates of Expected Phenomena G.E. TEMPO, RM62TMP-20, DA 49-146-XZ-036

[REDACTED]

[REDACTED]



3. Hypothesis 3

[Redacted text block]

These inhomogeneities will give rise to radar reflections. As the acoustic wave passes upward causing further turbulence, it (a) passes too high for the radar antenna pattern, and (b) causes turbulence in regions where turbulent scale sizes must be very large because of the large molecular mean-free paths.

[Redacted text block]

DNA
(b)(3)

a. Pro and Con Arguments

- (1) [Redacted list item]



[REDACTED]

b. Summary

Any hope that this hypothesis could explain the observed effects is rather well wrapped up in, at this time, undetermined numbers.

4. Hypothesis 4

Some predetonation calculations (see TEMPO⁺ and LASL⁺ predictions) suggested that debris from the weapon would travel and be stopped in a flat-bottomed manner at an elevation of the order of 200 km. Though post-detonation effects measurements seem not to confirm many of the predictions, a flat-bottomed debris pancake (which subsequently collapses back into the original field lines) could also give rise to a wave of some sort which travels in plane-wave fashion down into the reflecting region much as an X-ray produced wave of Hypothesis 3 traveled upwards. Such a wave again may produce inhomogeneities producing echoes.

D x A
(8) (5)

a. Pro and Con Arguments

[REDACTED]

b. Summary

At this time without additional data from other projects to draw upon we have not formed any opinions as to the validity of this hypothesis.

+ Loc. cit.

* Private Communication, H. Hoerlin, referring to report by R. W. Bussard, R. D. Cowan, "Bomb Plasma Expansion and Stopping in High Altitude Shots".

[REDACTED]

[REDACTED]

There must certainly be additional possible mechanisms which have not occurred to us at this time. It is very possible that, if one of our hypotheses is correct in the sense that the particular mechanism is in predominant control, other effects will alter magnitudes and locations of the radar echoes.

[REDACTED]

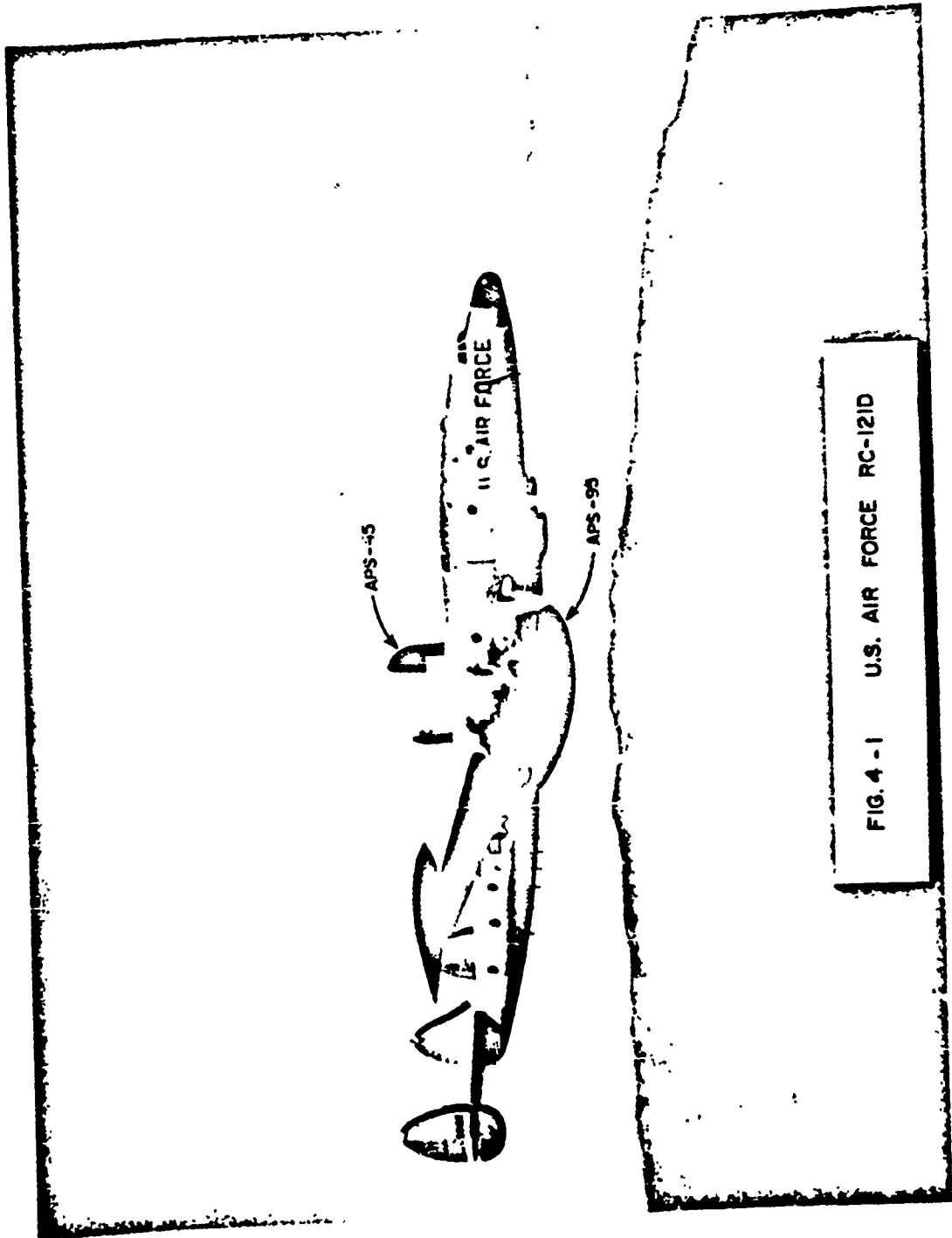


FIG. 4 - 1 U.S. AIR FORCE RC-121D

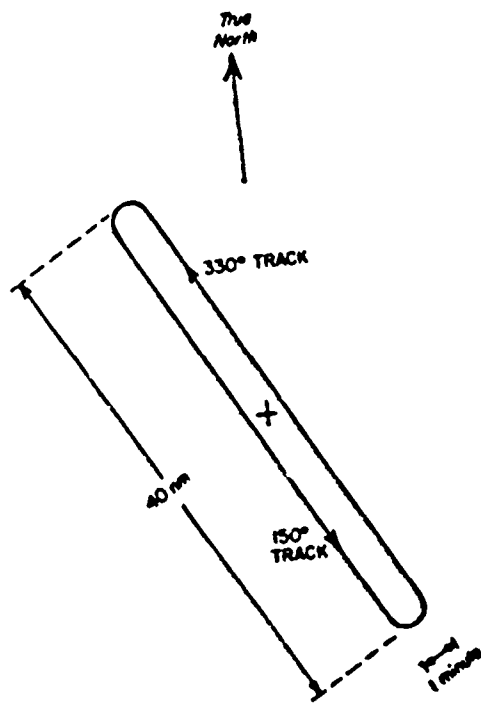


FIG. 4-4a
ABUSIVE I PATTERN

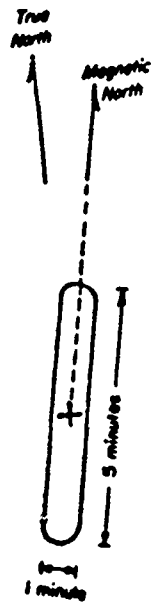


FIG. 4-4b
LAMBKIN I-4 PATTERN

PAGES 91-105 DELETED

TABLE 4-1

Parameters of the APS-95 Radar

Frequency	420 to 450 Mc
Peak power	1.5 Mw
Pulse width	6 to 9 μ sec
PRF	250 cps*
IF bandwidth	200 kc
Noise figure	8 db
MDS	-115 dbm
σ_{min} at 200 nm	$10 m^2$
Beamwidth	10 degrees--E plane** 18 degrees--H plane
Antenna rotation	6 rpm***
Dynamic range	20 db

* Normal prf is 320 cps

** Main beam is oriented 8.5 degrees down from airplane axis; however, plane generally lies 4.5 degrees nose-up, resulting in the main beam being 4 degrees down from horizontal

*** Antenna can also rotate at 1, 2, and 4 rpm



TABLE 4-11

LOCATIONS OF AIW AIRCRAFT

<u>Location Code</u>	<u>Code Name</u>	<u>Longitude</u>	<u>Latitude</u>
S0	Abusive 1	167°57.5' W	17°02' N
S1	Lambkin 2	165°36' W	10°54' N
S2	Lambkin 1	165°30' W	13°46' N
S3	Lambkin 3	169°00' W	8°48' S
S4	Lambkin 4	170°12' W	12°33' S





CHAPTER V CANTON ISLAND MEASUREMENTS

by

J.R. Hodges, L.T. Dolphin, Jr.

Observations and Results

As part of Project 6.9, SRI operated a simple 27-Mc radar and all sky camera at Canton Island during STARFISH PRIME. In addition, the project representative operating these equipments took some Ektachrome photographs of the visual phenomena, the success of which was due to experience in photographing natural auroral forms.

The radar, a type common in IGY backscatter research, has characteristics which are described in Table 5-I. The radar was operated for the STARFISH PRIME event and data recorded on magnetic tape for later analysis, which is not yet fully completed.

Geometry of the Canton Island Radar Post is sketched in Fig. 5-1. This sketch, together with the summary of radar events (Table 5-II), can be used to derive a qualitative radar picture of STARFISH PRIME as seen from Canton Island.

The basic radar data in the form of intensity-modulated, range-time records is presented in Figs. 5-2 through 6. Both long and short pulse data is shown. These figures will be most useful for qualitative examination, since Table 5-II contains a good chronology of the important events seen on the records. Fig. 5-7 is a range-time plot of observed echoes.

[REDACTED]

The radar phenomena observed are by no means completely understood at this time, and the authors present instead a few comments for the purpose of stimulating comments and discussion.

The absence of echoes on the radar prior to H +22 sec is consistent with the early-time absorption picture, and is well documented by riometers at Canton and elsewhere. The synchrotron noise observed by the radar receiver is also consistent with results reported elsewhere.

DVA
(b)(3)


[REDACTED] and it is possible that this echo arose from a confined, ascending tube of debris; echoes were seen perpendicular to that field which passes through the burst point.

[REDACTED]

Photographs of the visual phenomena are reproduced in Figs. 5-21 through 5-23 printed from the original High-speed, Daylight Ektachrome.

Table 5-111 describes the exposure conditions and camera position for each of these photographs.

[REDACTED]



An all-sky camera was also operated at Canton Island during the event. This type of camera, with "fish-eye" lens, provides an extremely wide field of view.

All-sky photographs (the originals are black and white) are presented as Figs. 5-8 through 20. The fine filamentary structures in the tube are evident. Note that the late-time brightness of the southern auroral area exceeds that of the northern end.

Fig. 5-34 shows the results of a densitometer tracing of the all-sky camera negatives.

PAGES 11-147 DELETED

[REDACTED]

TABLE 5-III
STARFISH PRIME CANTON COLOR PHOTOS

Taken by J. Hodges

<u>Figure</u>	<u>Camera Direction</u>	<u>Approximate Time Exposure Was Started</u>	<u>Approximate Exposure Time</u>
5-21	South	H + 0 sec	10 sec
5-22	North	H + 30	10
5-23	North	H + 45	15
5-24	South	H + 55	10
5-25	North	H + 115	10
5-26	North	H + 130	10
5-27	North	H + 170	10
5-28	South	H + 205	10
5-29	South	H + 315	10
5-30	South	H + 340	5
5-31	South	H + 350	3
5-32	South	H + 360	10
5-33	South	H + 370	10

Eastman 35mm Hi Speed Daylight Ektachrome, ASA 160, with regular development was used with a 50mm focal length lens, set at f/2.

[REDACTED]

CHAPTER VI JOHNSTON ISLAND EARTH-POTENTIAL RECORDS

An earth-potential recorder was operated during STARFISH PRIME at Johnston Island. This recorder consisted of long copper rods driven into the ground 200 feet apart. The rods paired magnetically north and south and magnetically east and west were connected to DC amplifier chains and pen chart recorders.

Figure 6-1 shows the earth-potential records during the event. After initially positive north and west potentials a long negative potential difference developed. These potentials were due to currents flowing in the earth, induced by similar currents flowing in the ionosphere. Since the recorder draws negligible current, it measures essentially the potential differences developed across points on the ground which resulted from the flow of these currents.

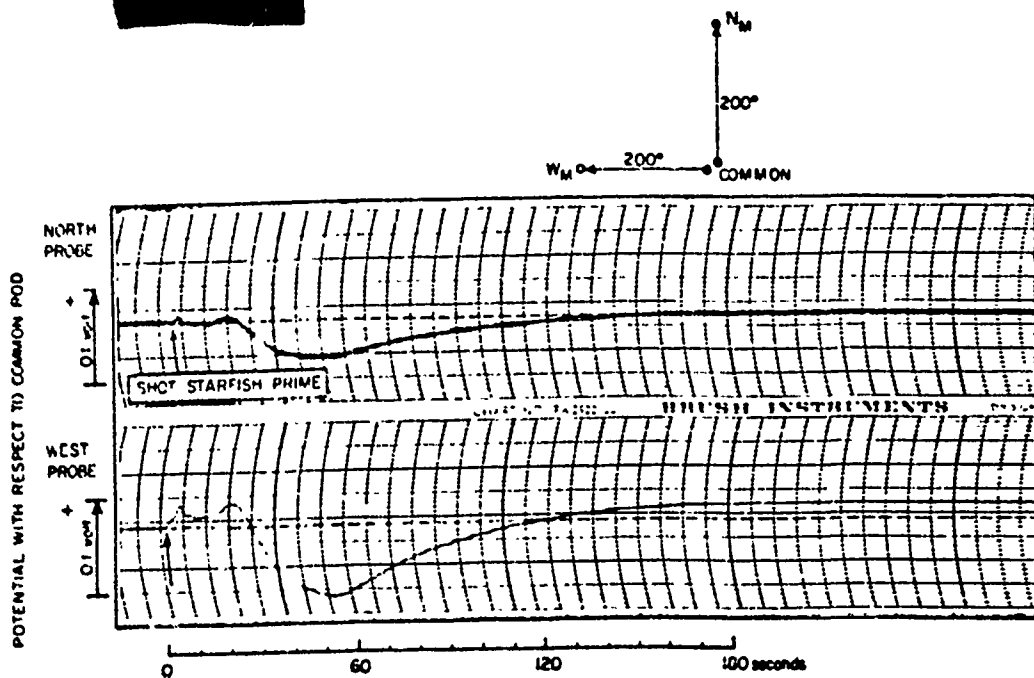



FIG. 6-1 EARTH-POTENTIAL ON JOHNSTON ISLAND DEVELOPED ACROSS 200-foot BASELINES

[REDACTED]

CHAPTER VII DAMP SHIP RESULTS

There are no results other than described in interim 72-hour reports by the Project 6.9 portion of Project 6.13 at this time. It is hoped that DAMP results will be made available to Project 6.8 in time for the POR.



CHAPTER VIII CONCLUSIONS

Although final conclusions cannot be drawn from the rather interim radar clutter results presented in this report, a number of comments concerning STARFISH PRIME can be made.

First, the results obtained indicate that none of the three models described in Chapter I for STARFISH PRIME are completely descriptive of the actual effects. The locations of the AEW aircraft was chosen to determine whether or not a debris "pancake" was formed, and if so, to what size. The relatively negative results indicate that such a "pancake" was not formed. Although the negative UHF results were in a way disappointing to project personnel, they are quite valuable to the understanding of the phenomena.

The relatively striking radar results from the ACANIA and the radar and visual Canton Island results indicate the considerable influence of the earth's magnetic field upon the radar echoes.

The lack of early time UHF radar clutter at Johnston Island indicate that the debris was spread in altitude over such a large extent that its effect in producing radar clutter was relatively weak.

Overall, the radar clutter results and associated experiments conducted during STARFISH PRIME were very successful. Final conclusion as to their significance must await further analysis and comparison with other projects results.

[REDACTED]

REFERENCES

1. V. L. Lynn and others; "Weapons Test Report of HARTACK Project 6.13"; Technical Memorandum No. 72, 13 April 1959; Lincoln Laboratory, Massachusetts Institute of Technology [REDACTED]

2. L. Dolphin and R. Dyce; "Operation HARTACK/NEWSREEL Radio Attenuation and Reflection Phenomena"; Final Report Part I, Contract AF 19(604)-3462, February 1960; Stanford Research Institute, Menlo Park, California; [REDACTED]

3. "Electromagnetic Blackout Guide, Volume II; DASA-1229, 1 May 1961; Contract DA 49-146-XZ-038; General Electric TEMPO, Santa Barbara, California; [REDACTED]

4. A. L. Lutter and R. E. Lelovier, "Pancake Shot"; RAND Research Memorandum RM-2361, April 1959; RAND Corp., Santa Monica, California; [REDACTED]

5. C. H. Cumuck and G.A.M. King, "Disturbance in the Ionospheric F-region Following the Johnston Island Nuclear Explosion," New Zealand Journal of Geology and Geophysics 2, pp. 634-641 (August 1959).